

GA-A26789

NUMERICAL ANALYSIS OF RESONANT MAGNETIC PERTURBATIONS FOR ELM CONTROL IN ITER

by

D.M. ORLOV, T.E. EVANS, R.A. MOYER, M.J. SCHAFFER, and O. SCHMITZ

JUNE 2010



DISCLAIMER

This report was prepared as an account of work sponsored by an agency of the United States Government. Neither the United States Government nor any agency thereof, nor any of their employees, makes any warranty, express or implied, or assumes any legal liability or responsibility for the accuracy, completeness, or usefulness of any information, apparatus, product, or process disclosed, or represents that its use would not infringe privately owned rights. Reference herein to any specific commercial product, process, or service by trade name, trademark, manufacturer, or otherwise, does not necessarily constitute or imply its endorsement, recommendation, or favoring by the United States Government or any agency thereof. The views and opinions of authors expressed herein do not necessarily state or reflect those of the United States Government or any agency thereof.

NUMERICAL ANALYSIS OF RESONANT MAGNETIC PERTURBATIONS FOR ELM CONTROL IN ITER

by

D.M. ORLOV,* T.E. EVANS, R.A. MOYER,* M.J. SCHAFFER, and O. SCHMITZ†

This is a preprint of a paper to be presented at the 37th European Physical Society Conference on Plasma Physics, June 21-25, 2010, Dublin, Ireland and to be published in the *Proceedings*.

*University of California-San Diego, La Jolla, California, USA.

†Forschungszentrum Juelich GmbH, IEF4-Plasma Physics, Juelich, Germany.

Work supported in part by
the U.S. Department of Energy
under DE-FG02-07ER54917 and DE-FC02-04ER54698

GENERAL ATOMICS PROJECT 30200
JUNE 2010

Numerical analysis of resonant magnetic perturbations for ELM control in ITER

D.M. Orlov¹, T.E. Evans², R.A. Moyer¹, M.J. Schaffer², and O. Schmitz³

¹*University of California San Diego, La Jolla, CA 92093, USA*

²*General Atomics, San Diego, CA 92186-5688, USA*

³*Forschungszentrum Juelich GmbH, IEF4-Plasma Physics, 52428 Juelich, Germany*

Resonant magnetic perturbations (RMPs) are used for the suppression and mitigation of edge localized modes (ELMs) in DIII-D [1] and other tokamaks. ELMs drive impulsive energy losses and can be detrimental to plasma facing surfaces in future ITER high power experiments. During RMPs the vacuum topology of the magnetic field, excluding the plasma response, changes producing a stochastic region that is formed by overlapping magnetic islands. Experiments have shown that the application of RMPs leads to increased transport in the pedestal and the suppression of Type-I ELMs. Understanding ELM physics and developing the ability to control Type-I ELMs will improve the performance and longevity of ITER plasma-facing surfaces in high energy density tokamak-based fusion confinement.

In this work we analyze the effect of the RMP coils on the magnetic topology in ITER since this is known to affect the stability of Type-I ELMs. The ITER RMP ELM control approach is based on the successful ELM suppression with DIII-D I-coils. Thus, by comparing the magnetic topology in DIII-D with that in ITER we can extrapolate our knowledge of the DIII-D RMP ELM suppression strategy to the future ITER experiments.

Previously, several preliminary ITER coil designs were studied for the coil mode spectra and magnetic island overlap [2,3]. In the present work we extended this research to the current design for the ITER internal RMP coils (shown in Figs. 1 and 2) using the newest ITER kinetic equilibria produced with the Corsica code [4]. We have also included the effect of the ITER Error Field Correction coils in the analysis, which has not been done in the earlier studies.

Our preliminary studies have shown that we can achieve the best RMP performance in ITER H-mode and steady state discharges using an $n=4$ waveform in the RMP coils. Two sets of current waveforms have been studied — square and cosine $n=4$

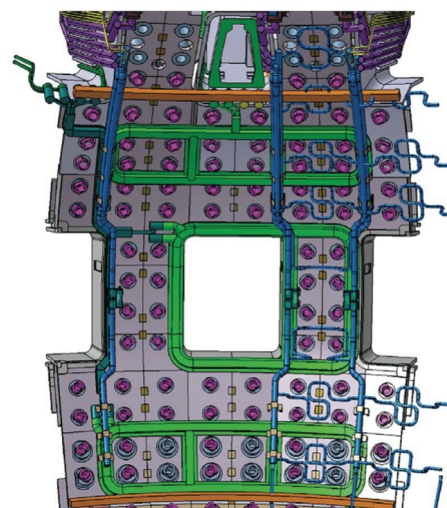


Fig.1. ITER RMP coils (shown in green).

waveforms. The square wave allows us to achieve maximum current amplitudes in the RMP coils thus creating larger magnetic islands and better Chirikov island overlap parameter. On the other hand, the cosine wave is better optimized for a smooth rotation of the external field for spreading of the localized heat and particle fluxes. The study also showed that the current of 50 kAt in the Error Field Correction coils produces negligible effect on Chirikov parameter and field line loss, but the maximum current of 150 kAt improves the field line loss below $\Psi_N=0.7$.

Figure 3 shows radial profiles for the Chirikov parameter and field line loss ratio in an ITER H-mode discharge with an $n=4$ 90 kAt square wave that has a 40° toroidal phase shift in the middle row of coils. The toroidal phase shift reinforces the return flux and allows for better alignment with the local magnetic field line pitch angle. The value of ψ_N at which the Chirikov parameter ≥ 1 in this case $\sigma_{\text{CHIR}} = 0.77$ exceeds the criteria for ELM suppression in DIII-D ($\sigma_{\text{CHIR}} = 0.835$). The complex shape of the Chirikov profile is due

to a large number of magnetic islands created by a square wave ($n=1,2,3,4,5$). The field line loss ratio is calculated using TRIP3D vacuum field line tracing code and is expressed as the ratio of field lines that hit the divertor to the total number of field lines started on a particular flux surface. Here we started 128 lines on each flux surface and traced the lines for 200 toroidal rotations. The results show that the field lines are lost from the plasma starting at $\Psi_N=0.7$, and that 90% of pedestal field lines are lost to the divertor in less than 200 toroidal rotations.

The 90 kAt $n=4$ cosine waveform also produces a broad field line loss profile which starts from $\Psi_N=0.8$, and creates a field line loss ratio of approximately 80% in the pedestal region. Although the cosine waveform produces a smaller field line loss profile when compared to

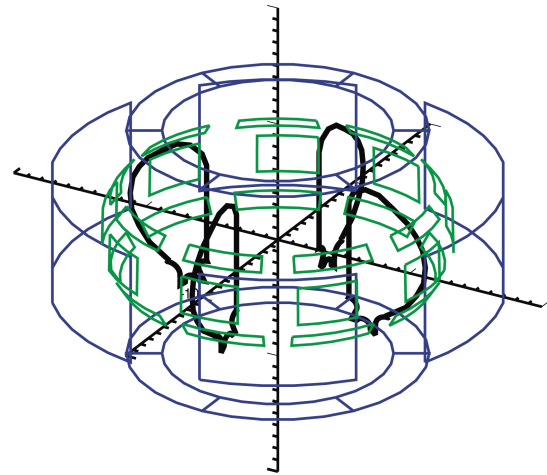


Fig. 2. ITER 3x9 RMP (green) and 3x6 EFC (blue) coil sets. ITER limiter is shown in black.

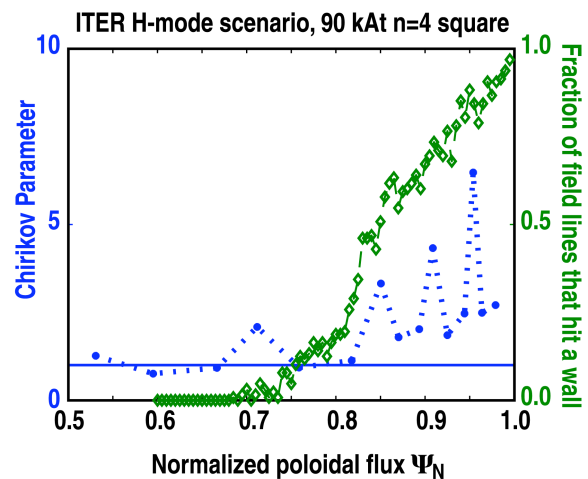


Fig. 3. Field line loss ratio (green) and Chirikov profiles (blue) for ITER H-mode discharge with RMP $n=4$ 90 kAt square wave.

the square wave of the same magnitude, it is still broader than the loss ratio found in a typical DIII-D RMP ELM suppressed discharge with an ITER similar shape (126006 at 3600 ms) using 4 kAt even parity I-coil currents (shown in Fig. 4).

The robustness of the square waveform is also beneficial in the event that some of the RMP coils fail in ITER. In our study we looked at how the characteristics of RMP ELM suppression change when one, two or three consecutive coils lose current. The results for the worst-case scenario (when three consecutive RMP coils fail in a single poloidal row) is shown in Fig. 5 in terms of the Chirikov parameter dependence on the toroidal position of failed coils. Here, the top row is the solid curve with open squares, the middle row is the dashed curve with solid circles and the bottom row is the dotted curve with open circles. The initial value of Chirikov parameter corresponding to fully operating RMP coil set ($\sigma_{\text{CHIR}} = 0.77$) is represented by the solid black line. The asymmetry in the results is due to the asymmetry of the $n=4$ square waveform fit into nine ITER RMP coils when the values of the currents in the ninth coil is identical to the values of the currents in the first coils (+ - + - + - + - +). As it can be seen, the biggest effect on the Chirikov parameter is produced by the failure of the middle row RMP coils where the Chirikov parameter $\sigma_{\text{CHIR}} \approx 0.81$. But even in this case, the Chirikov parameter is still in an acceptable range compared to the DIII-D value of $\sigma_{\text{CHIR}} = 0.835$ for RMP ELM suppression. It should be noticed that this coil failure scenario is producing an $n=1$ component, but its effect is negligible.

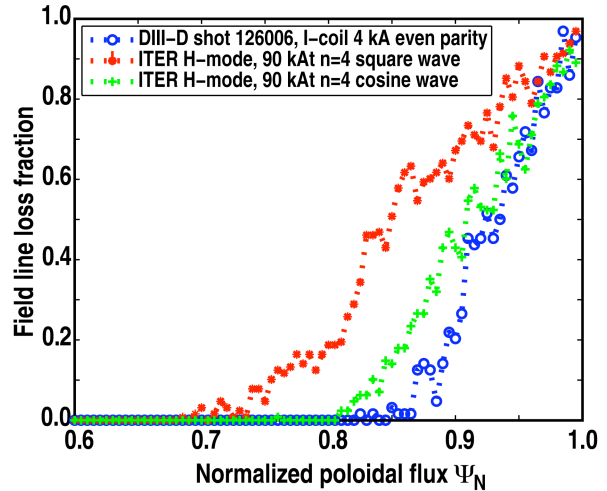


Fig. 4. Radial profile of field line loss ratio for ITER H-mode and DIII-D ISS discharges.

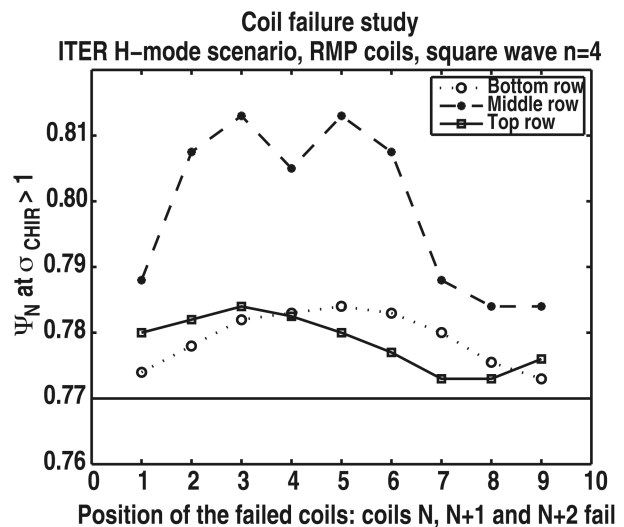


Fig. 5. Chirikov parameter in three-coil failure study for coil failure in top, middle or bottom row of RMP coil set.

Based on the results of vacuum models, we have modeled the magnetic footprint for the ITER ELM control coils [5]. The modeling was performed for $n=4$ 90 kAt square and cosine current distributions in the RMP coils. The results are shown in Fig. 6. The footprints at the inner strike line are shown on the left, and the footprints at the outer strike line are shown on the right. Top row figures correspond to the square waveform, and bottom row figure represent the cosine waveform. The dashed horizontal line in the figures represents the material transition from CFC to Tungsten. The magnetic footprint pattern is very similar to the one observed in DIII-D RMP ELM suppressed shots. As seen in Fig. 6, the outer tips of the lobes

connecting field lines from inner region of hot plasma can reach Tungsten area when 90 kAt $n=4$ square wave RMP is applied, and can channel hot particles onto surfaces that are heat flux sensitive. On the other hand, the lobes stay well inside the CFC domain when 90 kAt $n=4$ cosine wave current distribution is applied.

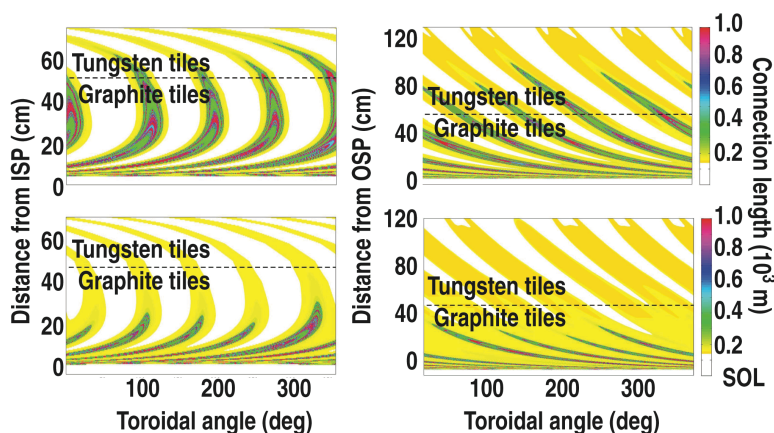


Fig. 6. Magnetic ITER divertor footprint pattern at inner (left) and outer (right) strike lines with $n=4$ RMP spectrum applied with square (top) and cosine (bottom) wave current distribution.

Overall, our study shows that the current design of ITER RMP coil set exceeds the DIII-D criteria needed for ELM suppression using either a square wave or cosine wave. The studied $n=4$ square and cosine waveforms show very good Chirikov parameter values and field line loss radial profiles for both H-mode and Steady-state operation in ITER. These configurations and current distributions are robust and show good characteristics over a range of RMP coil current amplitudes and phases. They also provide a significant operational margin in the event of up to 3 isolated coil loop failures.

This work was supported in part by the US Department of Energy under DE-FG02-05ER54809, DE-FG02-07ER54917, and DE-FC02-04ER54698. The authors would like to thank Dr. T.A. Casper for ITER equilibria.

- [1] Evans T.E., *et al.*, Nature Phys. **2**, 419 (2006)
- [2] Becoulet M., *et al.*, Nucl. Fusion **48** (2008)
- [3] Becoulet M., *et al.*, Nucl. Fusion **49** (2009)
- [4] Crotinger J.A., *et al.*, Rep. UCRL-ID-126284, LLNL, CA (1997)
- [5] Schmitz O., *et al.*, J. Nucl. Mater. (2010 submitted)